

## Numerical simulation of in situ exploitation of oil shale by injecting high-temperature steam

Dong Yang<sup>(a)</sup>, Yangsheng Zhao<sup>(a,b)\*</sup>, Zhiqin Kang<sup>(a)</sup>

<sup>(a)</sup> Key Lab of In-situ Property-improving Mining of Ministry of Education, Taiyuan University of Technology, Taiyuan, China 030024

<sup>(b)</sup> College of Mining Engineering, Taiyuan University of Technology, Taiyuan, China 030024

**Abstract.** *Oil shale has a very important strategic value for energy safety, but in situ pyrolysis technology still faces both scientific and technical problems that urgently need to be overcome. Among the current world's oil shale in situ conversion technologies, the Chinese in situ pyrolysis technique, which consists in injecting high-temperature water vapor, is considered to be one of the most efficient methods in this field. The thermal-hydraulic-mechanical-chemical (THMC) coupling model for this method is presented. Based on the model, the temperature distribution and permeability evolution were simulated. It was concluded that, first, due to the existence of prefracturing cracks, the pyrolysis front tended to be focused on both sides of the prefracturing cracks and the region had a relatively high temperature and permeability. Also, the pyrolysis front formed a sharp protrusion at the leading edge on both sides of the crack. Second, in the process of pyrolysis, pore-crack and tensile stress in the high-temperature region increased rapidly, and the permeability coefficient increased by 3–4 orders of magnitude and formed an in situ pyrolysis zone of oil shale. Third, the thermal protective, seepage insulation and stress trap zones were formed around the pyrolysis zone, and the internal boundaries of the three zones coincided, thus forming a good environment for underground pyrolysis similar to that of ground retorting.*

**Keywords:** *oil shale in situ pyrolysis, numerical simulation, pyrolytic zone evolution, trap zone.*

### 1. Introduction

Oil shale is a sedimentary mineral with rich kerogen that has been attracting energy and oil industries' attention worldwide for a long time already; the underground oil shale in situ retorting technology has been extensively studied. The in situ electric heating technology for oil shale was invented by Shell [1] and the Electrofrac™ in situ pyrolytic technology was developed by ExxonMobil [2]; however, neither of these technologies has been realized

\* Corresponding author: e-mail [y-s-zhao@263.net](mailto:y-s-zhao@263.net)

as commercial operations so far. Several companies in the United States use high-temperature air, high-temperature CO<sub>2</sub>, hydrocarbon gas, etc., for the pyrolysis of oil shale, but these approaches are still in the experimental stage [3]. Radiant heat technologies, such as microwave radiation, are yet more immature [4].

Many numerical simulation studies have been carried out on the above oil shale in situ mining technologies. The earliest investigations on the numerical simulation of in situ pyrolysis of oil shale, which were conducted by Braun et al. [5] and Braun and Burnham [6], date back already to the 1980s and 1990s. Burnham et al. [7] and Burnham [8] presented mathematical models for determining changes of the porosity and permeability of Green River Formation oil shale during retorting under confinement. When retorted unconstrained, numerous fractures are formed in oil shale due to the limited tensile strength of retorted rock, and the permeability increases from micro- or nano-Darcy levels to Darcy levels. In contrast, the fracture permeability is minor when constrained by lithostatic loads, which are typical of in situ retorting; thus, the permeability increases only to milli-Darcy levels. The investigators simulated the in situ electric heating scheme with a hole spacing of 16 m. After 400 days of heating, oil production began and in 700 days its peak reached 1.2 BBL oil/day. Moreover, heavy oil was the main component; light oil accounted only for a small portion of total oil, and oil had a gravity of 33 API. Fan et al. [9] used the coupled numerical simulation method with a thermal/compositional, chemical reaction flow to investigate how oil was produced and affected by the heater temperature and location. Hoda et al. [10] applied the numerical simulation method to obtain the long-term low-temperature retorting simulation of Electrofrac by using Colony Mine as an example and analyzed the temperature, voltage, current and rock deformation. Lee et al. [11] studied the effects of the temperature of vertical heaters and the spacing of hydraulic fractures, as well as the position of horizontal production wells on the in situ conversion on an example Electrofrac and Steamfrac processes. The applied in situ conversion processes, including Electrofrac with the short spacing of hydraulic fractures, showed good heating efficiency by completely decomposing kerogen in the system. Lee et al. [12] investigated the effect of oil shale matrix porosity, oil shale grade, and the spacing of the natural fracture network on hydrocarbon productivity and selectivity. Hui et al. [13] have been studying oil shale conversion numerical simulation for 6–8 years, and reported achieving 90% oil shale extraction. Kelkar et al. [14] studied the thermal-hydraulic-mechanical-chemical (THMC) coupling process of in situ electric heating of oil shale developed by the ExxonMobil company. Through this work, the distribution of temperature, pressure, kerogen, oil saturation and the permeability coefficient in different locations of electric heating was revealed. The simulation was carried out during more than 200 days, and its pyrolysis range was 4–5 m. Youtsos et al. [15] simulated shale oil extraction with in situ thermal upgrading by using an in-house code. The researchers found hot

gas injection to be a viable method. The reaction wave progression could be tracked solely by monitoring the thermal wave. The dimensionless depletion region length governed oil recovery by conduction heating. The numerical simulation of the leading edge movement characteristics of thermonuclear reactions in in situ pyrolysis and the upgrading of oil shale, through sensitivity analysis, was performed to ensure the transmission of the thermal front. The pressure and permeability coefficient were found to influence pyrolysis more than many other factors. Zhang and Parker [16] considered the heat transfer rate of oil shale fracture and matrix and determined the oil yield from oil shale of different particle sizes at different heating rates and different temperatures. Lee et al. [17, 18] studied the numerical simulation of in situ pyrolysis and the upgrading of oil shale through in situ steam flow in vertical cracks and the multi-section steam fracturing in a horizontal well system. The above analysis shows that the numerical simulation has mainly focused on oil shale in situ exploitation technology using electric heating, while studies on the numerical simulation of oil shale pyrolysis through fluid convective heating are completely lacking.

The oil shale in situ convective pyrolysis technology, which consists in injecting high-temperature water vapor for oil and gas recovery (MTI), was worked out by Zhao et al. [19] in 2005. After that, samples from seven oil shale mining zones in China were tested experimentally. The experiments included the thermogravimetric, pyrolysis-permeability, microscale pyrolysis-rupture and large sample pyrolysis tests. The latter was performed in a high-temperature high-pressure tank, hydraulic fracturing was carried out via the high-temperature steam test with large-size specimens ( $300 \times 300 \times 300$  mm), and an in situ pyrolysis experiment was done with lump samples (approximately 2.2 m in diameter) by injecting high-temperature water vapor. The composition and characteristics of oil and gas of pyrolyzed oil shale, as well as the feasibility of recycling and reusing the cooled and salinized vapor water were studied. Based on the above experiments, the permeability, elastic modulus, Poisson's ratio and gas production law of oil shale under high temperature were determined. However, there are still two problems to resolve. One is to elucidate whether the high-temperature fluid injected during the heat injection process will always be short-circuited only along the fracture crack channel, which would result in the failure of the mining process. The other problem is to determine the laws of temperature and pressure distribution and fluid migration of rock mass under in situ formation stress conditions. These two problems need to be solved not by traditional experimental methods, but through theoretical deduction and numerical simulation, which is the research subject of this paper.

For this purpose, the thermal-hydraulic-mechanical-chemical coupling model for in situ heating of oil shale is presented. This simulation process has two major novelties. First, all simulation parameters were obtained through previous experiments and are close to those used in engineering practice.

Second, steam and water are defined as two inseparable components and their mixture is treated as a single fluid medium with continuously changing physical composition. In addition, this simulation model can provide theoretical support for carrying out real in situ steam injection pyrolysis of oil shale and help predict more accurately the process temperature range as well as production lifespan.

## **2. THMC coupling model of the in situ pyrolysis of oil shale**

The core technical content of the MTI technology for oil shale in situ steam injection is as follows. First, the group wells are positioned on the ground and are drilled into the oil shale ore layer treatment interval using the group well hydraulic fracturing technology to ensure that the steam injection and production wells are connected. Then, superheated steam with a temperature higher than 500 °C is injected into the oil shale deposit along the steam injection well to heat the ore body so that the organic matter in the oil shale deposit is thermally decomposed to form oil and gas, and the oil and gas are carried from the production well via low-temperature steam. The production is discharged to the ground and then condensed to separate oil, gas and water to obtain the oil and gas products, respectively. In this paper, the laws of heat transfer, seepage, oil shale pyrolysis chemical reaction, oil shale pores evolution and deformation are studied in the complete process of oil shale exploitation, from the superheated steam injection into the injection well to the low-temperature steam and gaseous oil and gas production from the production well.

### **2.1. Basic assumptions**

The current study proceeds from the following basic assumptions:

- 1) Compared with heat injection steam and condensate water, the contents of oil shale oil and gas products are low, and the flow characteristics of fluid products can be neglected in model calculation.
- 2) The effect of surface tension at the interface between water and steam is neglected.
- 3) Regardless of the chemical reaction of pyrolysis and the pyrolysis time, the pore fracture rate is assumed to be a function of temperature.
- 4) Fluid pressure gradients and seepage rates in the reservoir with a small pressure gradient follow Darcy's law.
- 5) The local heat balance is instantaneously reached between the fluid and the solid, and it is considered that the temperature is the same at the same position.
- 6) Water vapor, water density, dynamic viscosity, thermal conductivity and specific heat are a function of temperature.

## 2.2. Mathematical model

The THMC coupling mathematical model of in situ heating pyrolysis of oil shale by injection of superheated vapor is put forward through a set of equations.

The rock mass deformation control equation can be expressed as follows:

$$(\lambda(T) + \mu(T))u_{j,ji} + \mu(T)u_{i,jj} + F_i - \beta_T T_{,i} - \alpha p_{,i} = 0. \quad (1)$$

The heat transfer equation for rock mass can be written as:

$$\rho_r C_{pr} \frac{\partial T_r}{\partial t} = \lambda_r T_{r,ii} + W_s. \quad (2)$$

The heat transfer equation for mixed gas is described as follows:

$$C_{pg} \frac{\partial(\rho_g T_g)}{\partial t} = \lambda_g T_{g,ii} - C_{pg} (\rho_g K_i p_{,i} T_g)_{,i} + W_g. \quad (3)$$

The mixed gas seepage equation is:

$$(k_i p_{,i}^2)_{,i} = \rho_g \frac{\partial p^2}{\partial t} + 2p_g \frac{\partial e}{\partial t} + W_o(T). \quad (4)$$

The explanations for physical quantities used in equations are given in the nomenclature. The presented model uses some terms which have been obtained from experiments, as shown below:

1) Permeability is the function of volume stress  $\Theta$  and temperature  $T$  [20]:

$$K_i = 5 \times 10^{-6} \text{EXP}(0.00310\Theta + 0.0106T). \quad (5)$$

2) The effective stress coefficient ( $\alpha$ ) of pore gas in oil shale is the function of temperature [20]:

$$\begin{cases} \alpha = 0 & T < 100 \text{ }^\circ\text{C} \\ \alpha = a \text{EXP}(b(T - 100)) & T > 100 \text{ }^\circ\text{C} \end{cases} \quad (6)$$

3) The heat capacity coefficient of mixed gas ( $C_{pg}$ ) is the function of the partition ratio of water vapor to pyrolyzed oil and gas:

$$C_{pg} = S_{wg} C_{pwg} + S_{og} C_{pog}. \quad (7)$$

4) Young's modulus  $E$  of rock is the function of temperature [21]:

$$E = 5254.5 - 618.35 \ln T. \quad (8)$$

5) Poisson's ratio  $\nu$  is the function of temperature:

$$\nu = 0.448 - 0.00039T. \quad (9)$$

6) The quality of gas pyrolyzed from kerogen is the function of volume stress and temperature:

$$\begin{cases} W_0 = 0 & T < T_{c1}, \text{ and } T > T_{c2} \\ W_0 = 3.3 \times 10^{-6} e^{(0.031\Theta + 0.0106T)} & T_{c1} < T < T_{c2} \end{cases}. \quad (10)$$

7) The density of mixed gas is the function of the partition ratio of water vapor to pyrolyzed oil and gas:

$$\rho_g = S_{wg} \rho_{wg} + S_{og} \rho_{og}. \quad (11)$$

### 3. Physical model simplification of the numerical simulation

The rock formation profile in the numerical simulation is shown in Figure 1. Three rock formations were considered in the model. From bottom to top, the formation consists of the floor from 0 to 40 m, oil shale from 40 to 80 m and the roof from 80 to 100 m. Two fractures zones located at 50–50.5 m (with an aperture of 0.5 m) and 60–60.4 m (with an aperture of 0.4 m) are set up in the oil shale formation to simulate hydraulic fracture induced fracture zones.

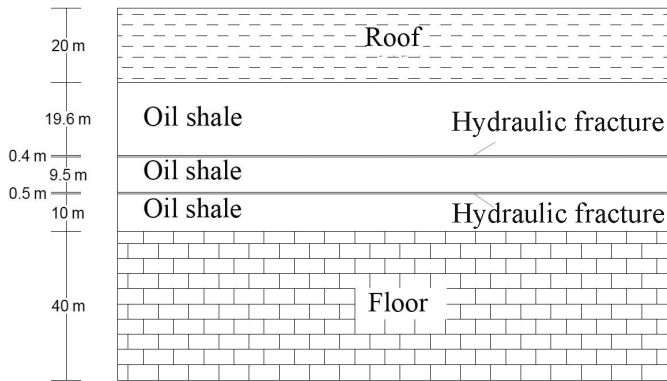


Fig. 1. Rock formation profile in the numerical simulation structure.

Normally, the simplest MTI technology system includes nine wells that are arranged in a square grid, as shown in Figure 2. One well in the centre is set as the heat injection well, and the other eight wells are production wells. All the wells have casing pipes and are sealed tightly with the surrounding rock, and when it is in an oil shale formation, the screen pipe is used alternatively to let only hot vapor transfer along the ore bed. In the simulation, the distance between the two wells is 40 m. Due to the geometry symmetry, only a quarter of the model was selected for calculation. The heat injection well is an interval between coordinates (0,0,40) and (0,0,80), as shown in Figure 3. The final simplified model and boundary conditions of solid deformation are shown in Figure 3.

The other boundary and initial conditions are summarized below.

The initial and boundary conditions of the heat field are:

- The initial temperature of the oil shale formation is:  $T(x, y, z, t = 0) = 20\text{ }^{\circ}\text{C}$ .
- The temperature of the ground surface is:  $T(x, y, z = 100, t) = 20\text{ }^{\circ}\text{C}$ .
- The boundary in which  $x = 0$  and  $y = 0$  is an adiabatic boundary.
- The temperature of the heat injection well is  $550\text{ }^{\circ}\text{C}$  for a given temperature.
- The floor boundary is an adiabatic boundary.

The initial and boundary conditions of the seepage field are:

- The initial pore pressure of the rock strata is:  $p = 0 \frac{\text{kg}}{\text{cm}^2}$ .
- The injection well is set at a fixed flow rate:  $q(t) = 1 \times 10^3 \text{ cm}^3/\text{s}$ .
- The production well is set with fixed pressure:  $p = 2 \frac{\text{kg}}{\text{cm}^2}$ .
- At the boundary where  $x = 0$  and  $y = 0$ , there are impermeable boundaries.
- The roof and floor are composed of a mudstone stratum with impermeable boundaries.

The initial boundary conditions of the solid stress field are:

- The gravity is considered in the calculation.
- At the surface  $z = 0$ ,  $w = 0$ ; at the surface  $x = 1$  and  $x = 150$ ,  $u = 0$ ; at the surface  $y = 0$  and  $y = 150$ ,  $v = 0$ .
- The top of the model is the ground surface.

To facilitate the discussion of the numerical simulation results, two sections were selected to analyze the calculation results. Section I is at section Y-Z where  $x = 0$ , and section II is a vertical section where  $x = y$ .

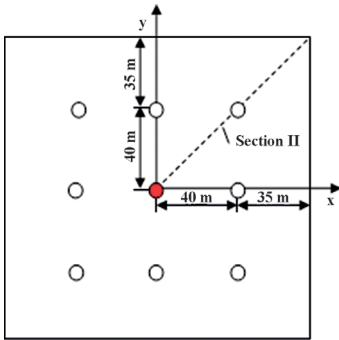


Fig. 2. Well distribution.

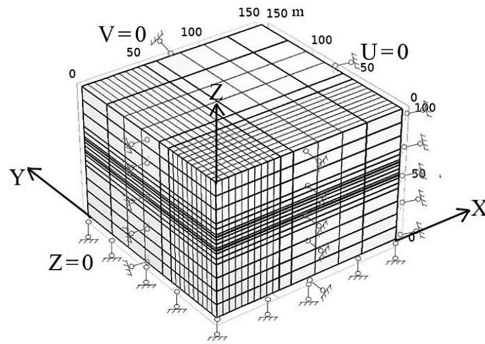


Fig. 3. Simplified model and boundary conditions of solid deformation.

### 3.1. Solution method of the coupled model

Based on the equations of the coupled mathematical model of temperature, seepage and solid deformation listed above, the Galerkin finite element method is used to derive a discrete form of each physical equation. The model is segmented using a spatial hexahedron 8-node isoparametric list, as shown in Figure 3. In the meshing, the method of combining the coarse and fine meshes is adopted, and the grid is dense in the vicinity of the heating and production wells and the oil shale deposit. This meshing method not only greatly improves the accuracy of calculation, but also eliminates the deviation

caused by improperly selected boundary conditions, which has a significant impact on the long-term extraction area and the heat recovery after extraction. The difference method is used to calculate the time. The initial time step is 10 seconds and the acceleration factor is 1.05. Repeated calculations verify that the difference method gives reliable results.

### 4. The simulation results and analysis

#### 4.1. Seepage field analysis

Figure 4 shows the contour map of the gas pressure of sections I and II at different pyrolysis times. From the figure one can see that in the ore bed in the region 10 m away from the heat injection well, the pressure gradient of the steam is larger and decreases very quickly. The pressure of the heat injection well decreases from 2.3 kg/cm<sup>2</sup> to 1.2 kg/cm<sup>2</sup> rapidly, and the steam pressure near the production well decreases to 1.05 kg/cm<sup>2</sup>. Along the oil shale seam, steam basically flows rapidly and mainly in the horizontal layer, which is used to pyrolyze the ore bed. In the roof and floor, steam flows slowly, the highest pressure being 1.2 kg/cm<sup>2</sup>.

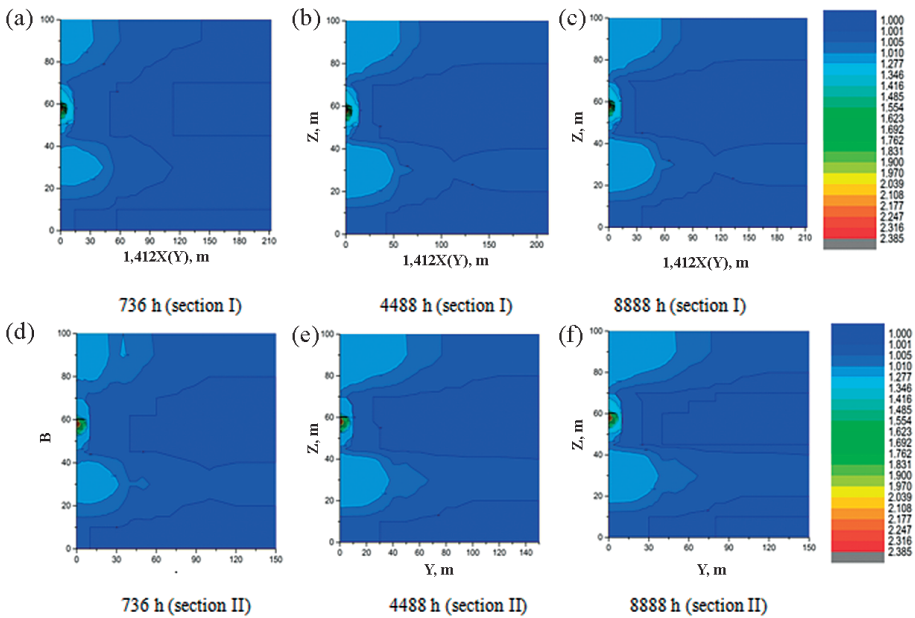


Fig. 4. Pore pressure contour map of selected sections during the pyrolysis process (kg/cm<sup>2</sup>) of section I: section Y-Z at X = 0; (b) section II: section X-Y at Z = 0.

## 4.2. Evolution of the temperature distribution

Figure 5 shows the temperature distribution of section II during the pyrolysis process by the injection of steam at different times.

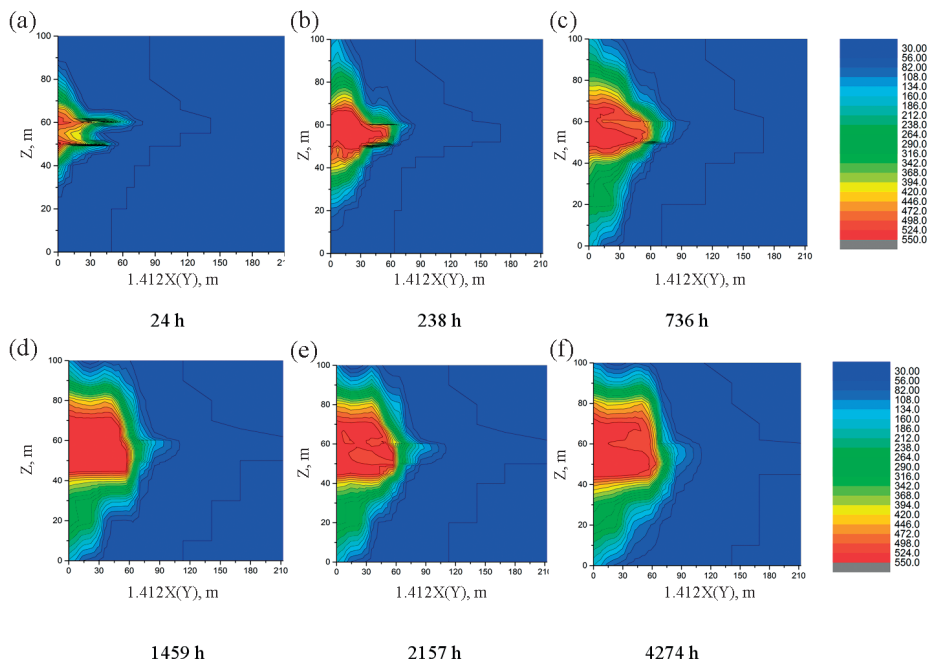


Fig. 5. Contour map of the temperature of section II during steam injection, °C.

It is clearly seen from Figure 5 that after having been injected for 24 hours, steam mainly flows along two prefractured fractures and forms a high temperature zone of oil shale heating, and this zone is also the crack area connected to the heat injection and oil production wells. In most parts of this zone, the temperature is above 460 °C, which means that in this zone, kerogen started to be pyrolyzed. At the boundary of the zone, there are formed two high-temperature-gradient zones with a cusped appearance. Within 30 m from the injection well, the temperature is reduced from 530 °C to 436 °C. At the production well, the temperature is decreased to approximately 50 °C within 30 m, and a large temperature decreasing gradient also forms on both sides and at the tip of the cracks. This shows that the technology of in situ pyrolysis of oil shale by injection of steam could produce pyrolysis oil and gas once the steam reaches the oil shale formation.

After approximately 10 days of steam injection, a high temperature pyrolysis region forms between two prefractured fractures between the area of the heat injection well and the production well, and the temperature can reach 530 °C. In the area 5 to 10 m from the heat injection well and outside the two cracks, a large temperature decrease gradient exists since in such

areas heat can only transfer by a conduction method; thus, the temperature is decreased from 530 °C to approximately 100 °C rapidly with a temperature gradient of  $-43$  °C/m. Within 30 m from the injection well to the production well and 10 m from the top and bottom, the temperature is approximately 530 °C, which means that oil shale is pyrolyzed steadily and quickly in this area. At a distance of 10 m from this area, the temperature is reduced from 530 °C to 410 °C, which is the initial pyrolysis or prepyrolysis region. Within 20 m outside the region, the temperature decreases from 410 °C to 80 °C rapidly, and the temperature gradient is 15 °C/m.

After 1 month of steam injection, the high temperature zone between the heat injection well and the production well not only continues to expand between the two fracturing cracks so that its minimum temperature rises to 498 °C, but also reaches the layer roof and the bottom plate on both sides of the expansion, and the temperature decreases from 550 °C to 500 °C in the area that extends to the 5 m bottom plate and 8 m roof areas. The area is a stable distillation area for oil shale. Due to heat conduction, the temperature decreases from 400 °C to 140 °C, and the cooling gradient is 6.5 °C/m; the outer side of the pyrolysis area of the ore layer and the top bottom plate expand to form an insulating belt that is approximately 20 m wide, and the temperature reduction gradient in the band is 25 °C/m.

From the temperature distribution at 2, 3 and 6 months after steam injection, we can clearly see the following. First, because of the drainage of the production well, the heat injection impact area does not extend to the distance along the ore layer. Second, the high-temperature zone gradually expands to the layer roof, spreading in the bottom plate direction at 3 months and reaching 72–80 m within the layer roof side. In this range, the temperature is reduced from 540 °C to 440 °C, and within 46–40 m from the layer floor it decreases from 540 °C to 420 °C. From 3 to 6 months, the expansion range of the 530–550 °C pyrolysis area is not too large because the positions of the production well and two fracturing cracks hinder the high-temperature steam flow, which slows the heat transfer. Third, the above phenomenon shows that only through regulation is a smooth steam flow achieved. To attain a rapid nondead end of the heating and efficient layer pyrolysis, this control method includes the real-time closure of the near-production wells and the opening of the distant production well drainage. Fourth, from the results obtained 6 months after steam injection pyrolysis, the fracturing cracks in the orebody have an obvious effect on the diversion steam in the early stage, which is very important for the connection of heat injection and production wells and the realization of smooth initial mining. In the initial mining period of approximately 20 days, oil shale is first pyrolyzed at two fracturing cracks and the junction and then the process gradually expands to the whole ore layer. With the exception of the first few days after steam injection, the pyrolysis can occur due to heating along the cracks; after that, there is a relatively uniform heating along the ore layer, steam outflows along the cracks directly from

the heat injection well to the production well. The reason for this difference is that once the oil shale orebody begins to be pyrolyzed, it will form highly developed pores and fissures and will constantly produce new steam migration channels.

### 4.3. Deformation and displacement of the ore bed during the pyrolysis process

Figure 6 shows the displacement changes of oil shale after heating for 4274 and 7678 hours, respectively. The figure reveals that a large compression deformation zone is formed in the ore bed and on the roof during the pyrolysis of oil shale. The maximum uplift displacement on the roof occurs at 8 mm at 7678 hours, and the width of the surface uplift area of the model is 120 m.

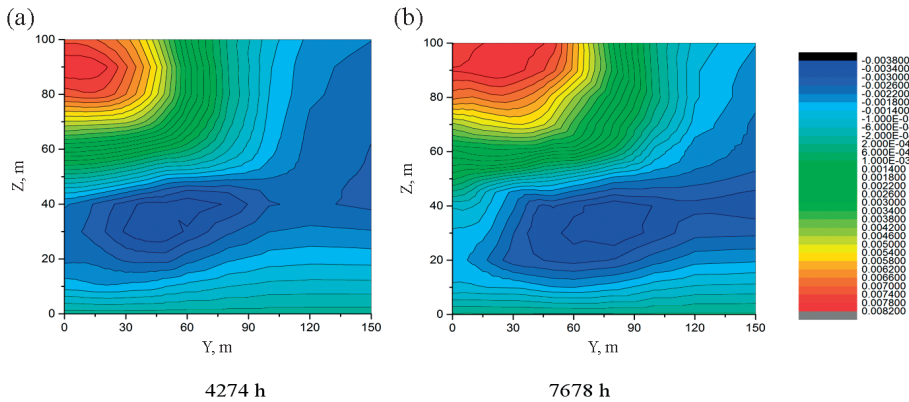


Fig. 6. Contour map of oil shale displacement during pyrolysis, m.

Figure 7 shows the vertical stress change of the ore layer. The shape and size distribution of the area where the stress changes drastically is very similar to that of the temperature field distribution. At a high temperature, 550 °C, the tensile stress is 10 MPa, and the temperature has a sharply attenuated band (i.e. the heat-insulating zone); on the outside, in the range of 30–40 m, the corresponding tensile stress is sharply reduced from near to far. The high tensile stress is greatly reduced to zero with a high stress gradient. If this band of sharply reduced stress is also considered to be an extension of the thermal insulation zone in the field of solid deformation, it can be said that the solid stress of the thermal insulation zone is 1.5 times wider than that of the thermal insulation zone. The compressive stress outside the band of the heat insulation zone gradually reaches the level of self-heavy stress from zero.

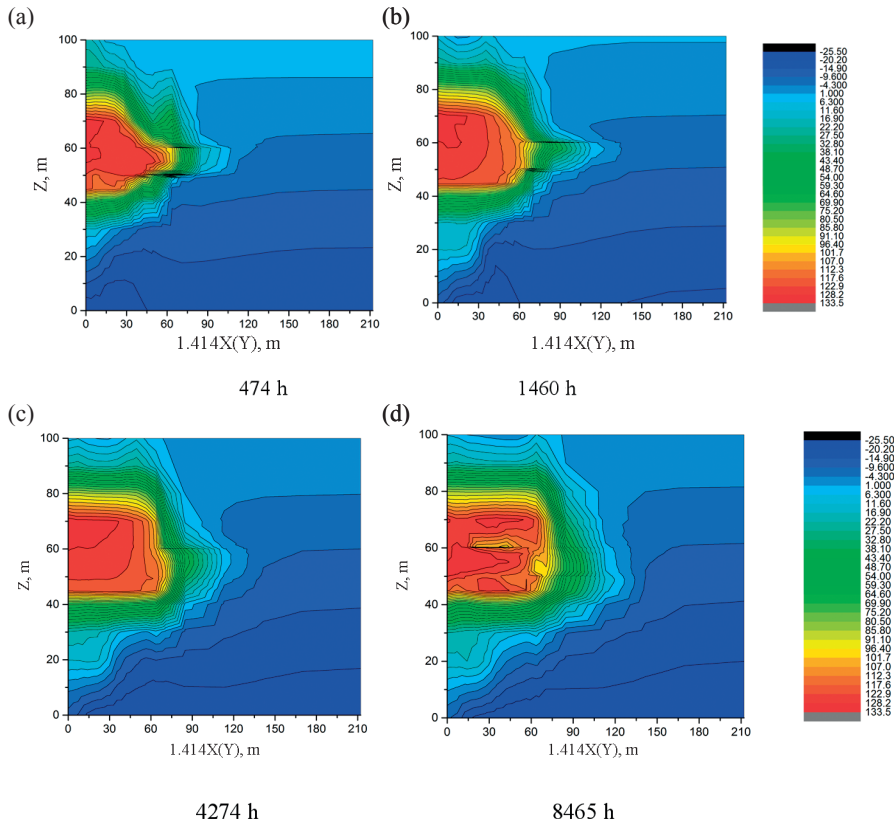


Fig. 7. Variation of the vertical stress in oil shale during pyrolysis.

#### 4.4. Analysis of evolution of the permeability coefficient in the pyrolysis process

Figure 8 shows the evolution of the permeability coefficient of oil shale during the in situ pyrolysis process. From the figure it can be seen that in the high-temperature pyrolysis zone, the permeability coefficient reaches 0.01 cm/s. In the heat insulation zone, which constitutes a closed loop of oil shale in situ pyrolysis, the permeability coefficient is reduced from 10–4 cm/s to 10–7 cm/s. In the roof and floor, the thickness of the closed band is approximately 10 m, and in the oil shale deposit, the width is approximately 30 m. From the construction of the underground in situ retorting zone to the trapping of the retorting zone, it is clearly indicated that the sealing of the roof and floor is tighter and its thickness is approximately 10 m, which evidences more obviously that the extremely weak leakage in the roof and floor causes a small heat loss by the steam retorting of oil shale. It can be seen from Figure 5 that the temperature of the roof and floor is lower than 400 °C, and the permeability of oil shale is lower at 400 °C, according to literature. In addition, Figure 7

displays that the roof and floor are in the compressive stress zone, and the compressive stress reduces the permeability. Therefore, the distribution of stress and temperature indicates the distribution of low permeability in oil shale.

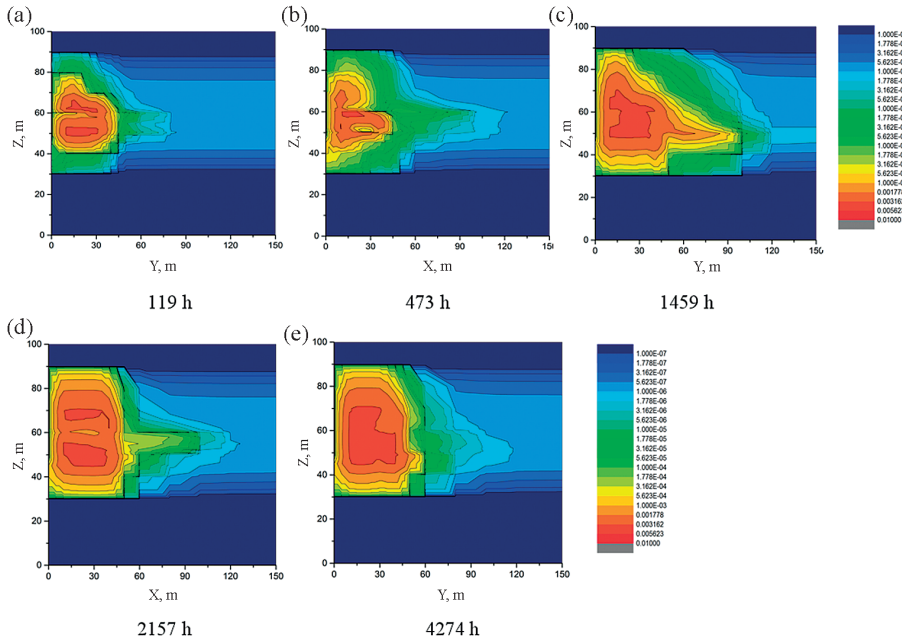


Fig. 8. Evolution of the permeability coefficient during the pyrolysis of oil shale.

### 5. Analysis and discussion of the in situ pyrolysis of oil shale by injection of water vapor

Based on the above analysis, the characteristics of the trap zone of oil shale in situ pyrolysis are listed in the Table. It can be seen from the Table that the trap zone of the oil shale pyrolysis zone is characterized by a wide stress zone, which indicates that the dense solid deformation will propagate further, but this propagation has no effect on in situ retorting. The heat insulation zone is narrower, and the permeability barrier zone is the narrowest. Within 20 m, the top and bottom plates have a temperature above 300 °C, forming a temperature barrier in this range. As is known, the permeability will only increase when the temperature is high, 400 °C. Considering that the stress compression is larger and above 400 °C the range is smaller, the permeability barrier zone is the narrowest.

**Table. The scale of different trap zones of the oil shale in situ pyrolysis**

Trap	Thermal traps	Seepage traps	Stress traps
Width, m	20	10	30–40

The analysis of numerical simulation demonstrates that by injection of steam the in situ convection heating of oil shale occurs. The process is similar to building a large retorting furnace underground in situ. Within the pyrolytic ore layer, the temperature above 500 °C is evenly distributed and the flow resistance is very low. Beyond the range of approximately 20–30 m, a heat insulation zone or a permeability barrier zone is formed. In this numerical simulation, a cubic area with a side length of 40 m and a height of 40 m is formed between the injection well and the production well, and the area contains 147,000 tons of ore bodies. The oil recovery per ton of oil shale is calculated to be 4% and the area could produce 5,000 tons of shale oil. A heat injection well covers 4 similar cubic areas, and 20 thousand tons of shale oil could be extracted. In practical engineering, production wells and heat injection wells are more than 80 m apart. This means that the pyrolysis region comprises 235 million tons of ore, and 94.2 thousand tons of shale oil can be extracted, which can be compared with a retorting chemical plant on the ground with an annual output of 100 thousand tons of shale oil. However, the advantages of this approach in terms of investment, environmental protection, cost effectiveness, etc., outweigh the pros of ground retorting.

## 6. Conclusions

In this paper, the laws of temperature, seepage, deformation and the stress field of the ore layer and the surrounding rock during the pyrolysis of water vapor in the case of prefracturing connection have been studied in detail, and the following conclusions can be drawn:

1. A coupled numerical simulation method for heat transfer, seepage, pyrolysis chemical reaction, and the deformation of convective heating is proposed.
2. When fracturing fractures exist, the early steam seepage and heat transfer spread through the cracks to both sides of the crack. The pyrolysis front always exhibits distinctive protrusion characteristics of high-temperature and high-permeability areas at the leading edge and on both sides of the crack.
3. In the process of pyrolysis, the oil shale pore and fractures extending rapidly from fractures to the oil shale mass around the fracture form a pyrolysis zone, and compressive stress in this area transforms rapidly into tensile stress. The permeability coefficient of the pyrolysis zone is increased by 3 to 4 orders of magnitude, thereby forming a fast and efficient pyrolysis region similar to the one in the ground retorting furnace.

4. In the in situ pyrolytic convection heating of oil shale by injection of steam, a high-temperature pyrolysis area is formed around the heat injection and production wells and the control section of the steam injection layer, which is surrounded by the heat insulation, stress concentration and impermeability barrier zones. The width of the heat insulation zone is approximately 20 m and that of the impermeability barrier zone is about 10 m; the stress trap zone is 30–40 m wide. The positions of the inner boundaries of the three zones are approximately the same.

## Nomenclature

$\rho_{og}$	density of pyrolysis gas, $\text{kg/m}^3$	$S_{wg}$	the relative saturation of water vapor in mixed gas, %
$\rho_g$	density of mixed gas, $\text{kg/m}^3$	$S_{og}$	relative saturation of pyrolysis oil and gas in a unit mass of gas, %
$\rho_r$	density of rock, $\text{kg/m}^3$	$C_{pr}$	specific heat of rock mass at constant pressure, $\text{J(g}\cdot\text{K)}$
$\rho_{wg}$	density of water vapor, $\text{kg/m}^3$	$p$	pore pressure, MPa
$\lambda_g$	thermal conductivity of mixed gas composed of water vapor and pyrolysis gas, $\text{W/(m}\cdot\text{K)}$	$C_{pg}$	heat capacity coefficient of mixed gas composed of vapor
$\lambda_r$	thermal conductivity of rock mass, $\text{W/(m}\cdot\text{K)}$ , $\text{J(m}^2\cdot\text{s)}$	$C_{pog}$	heat capacity coefficient of pyrolysis gas, $\text{J/g}$
$\lambda_r$	thermal conductivity of rock mass, $\text{J(m}^2\cdot\text{s)}$	$C_{pwg}$	heat capacity coefficient of water vapor, $\text{J/g}$
$\beta_T$	thermal expansion coefficient of rock obtained from experiment	$E$	Young's modulus, obtained from experiment, MPa
$\alpha$	effective stress coefficient of pore gas in oil shale, obtained from experiment	$W_g$	thermal sources or sink item of pore gas
$n$	rock porosity	$W_r$	thermal source of heat transfer of rock mass

$\Theta$	volumetric stress, MPa	$W_0(T)$	quality of gas pyrolyzed from kerogen, obtained from the experiment, $\text{kg}/(\text{m}^3 \cdot \text{K} \cdot \text{s})$
$\nu$	Poisson's ratio, obtained from experiment	$W_s$	source sink term of heat transfer of rock mass
$\lambda(T), \mu(T)$	Lami constant, is a function of temperature	$T_{,i}$	temperature gradient in $i$ direction
$K_i$	permeability, m/s	$F_i$	external force in $i$ direction
$T_g$	gas temperature, °C	$u_i$	displacement in $i$ direction
$T_r$	temperature of rock, °C	$u_j$	displacement in $j$ direction
$t$	time, h	$p_{,i}$	partial derivative of pore pressure
$e$	volumetric strain	$k_i$	permeability in $i$ direction
		$w$	water

## Acknowledgments

This work was funded by the National Natural Science Foundation of China (Grant Nos. 11772213 and U1261102).

## REFERENCES

1. Ryan, R. C., Fowler, T. D., Beer, G. L., Nair, V. Shell's in situ conversion process – From laboratory to field pilots. *ACS Sym. Ser.*, **1032** (Ogunsola, O. I., Hartstein, A. M., Ogunsola, O., eds.), Oxford University Press, 2010, 161–183.
2. Crawford, P. M., Killen, J. C. New challenges and directions in oil shale development technologies. In: *Oil Shale: Solutions to the Liquid Fuel Dilemma* (Ogunsola, O. I., Hartstein, A. M., Ogunsola, O., eds.), *ACS Sym. Ser.*, **1032**, 2010, 21–60.
3. Tanaka, P. L., Yeakel, J. D., Symington, W. A., Meurer, W., Spiecker, P. M., Del Pico, M., Thomas, M., Sullivan, K., Stone, M. Plan to test an in situ planar

- heater on a proposed RD&D Lease. *Proceedings of the 31st Oil Shale Symposium*. Golden, CO, Colorado School of Mines, 17–19 October 2011, 1–13.
4. El Harfi, K., Mokhlisse, A., Chanâa, M. B., Outzourhit, A. Pyrolysis of the Moroccan (Tarfaya) oil shales under microwave irradiation. *Fuel*, 2000, **79**(7), 733–742.
  5. Braun, R. L., Diaz, J. C., Lewis, A. E. Results of mathematical modeling of modified in-situ oil shale retorting. *Soc. Petrol. Eng. J.*, 1984, **24**(1), 75–86.
  6. Braun, R. L., Burnham, A. K. Mathematical model of oil generation, degradation, and expulsion. *Energ. Fuel.*, 1990, **4**(2), 132–146.
  7. Burnham, A. K., Switzer, L., Day, R. L., McConaghy, J., Hradisky, M., Coates, D., Smith, P., Foulkes, J., La Brecque, D., Allix, P., Wallman, H. Initial results from the AMSO RD&D pilot test program. *Proceedings of the 32nd Oil Shale Symposium*. Golden, CO, Colorado School of Mines, 15–17 October 2012.
  8. Burnham, A. K. Porosity and permeability of Green River oil shale and their changes during retorting. *Fuel*, 2017, **203**: 208–213.
  9. Fan, Y., Durlowsky, L., Tchelepi, H. A. Numerical simulation of the in-situ upgrading of oil shale. *Soc. Petrol. Eng. J.*, 2010, **15**(2), 368–381.
  10. Hoda, N., Fang, C., Lin, M. W., Symington, W. A., Stone, M. T. Numerical modeling of ExxonMobil's Electrofrac field experiment at Colony Mine. *Proceedings of the 30nd Oil Shale Symposium*. Golden, CO, Colorado School of Mines, 18–20 October 2010, 1–13.
  11. Lee, K. J., Moridis, G. J., Ehlig-Economides, C. A. Numerical simulation of diverse thermal in situ upgrading processes for the hydrocarbon production from kerogen in oil shale reservoirs. *Energ. Explor. Exploit.*, 2017, **35**(3), 315–337.
  12. Lee, K. J., Moridis, G. J., Ehlig-Economides, C. A. In situ upgrading of oil shale by Steamfrac in multistage transverse fractured horizontal well system. *Energ. Source. Part A*, 2016, **38**(20), 3034–3041.
  13. Hui, H., Ning-Ning, Z., Cai-Xia, H., Yan, L., Qing-Yong, L., Na, D., Xiao-Yan, H. Numerical simulation of in situ conversion of continental oil shale in Northeast China. *Oil Shale*, 2016, **33**(1), 45–57.
  14. Kelkar, S., Pawar, R., Hoda, N. Numerical simulation of coupled thermal-hydrological-mechanical-chemical processes during in situ conversion and production of oil shale. *Proceedings of the 31st Oil Shale Symposium*. Golden, CO, Colorado School of Mines, 17–19 October 2011, 1–8.
  15. Youtsos, M. S. K., Mastorakos, E., Cant, R. S. Numerical simulation of thermal and reaction fronts for oil shale upgrading. *Chem. Eng. Sci.*, 2013, **94**, 200–213.
  16. Zhang, F., Parker, J. C. An efficient modeling approach to simulate heat transfer rate between fracture and matrix regions for oil shale retorting. *Transport Porous Med.*, 2010, **84**(1), 229–240.
  17. Lee, K., Moridis, G. J., Ehlig-Economides, C. A. Oil shale in-situ upgrading by steam flowing in vertical hydraulic fractures. *SPE Unconventional Resources Conference, 1–3 April 2014, The Woodlands, Texas, USA*. Society of Petroleum Engineers, 2014, 1–13.
  18. Lee, K. J., Moridis, G. J., Ehlig-Economides, C. A. A comprehensive simulation

- model of kerogen pyrolysis for the in-situ upgrading of oil shales. *Soc. Petrol. Eng. J.*, 2016, **21**(5), 1612–1630.
19. Zhao, Y. S., Feng, Z. C., Yang, D. et al. *The Method for Mining Oil & Gas from Oil Shale by Convection Heating*. China Invent Patent, CN200510012473, April 20, 2005.
  20. Kang, Z. Q. *The Pyrolysis Characteristics and In-Situ Hot Drive Simulation Research That Exploit Oil-Gas of Oil Shale*. PhD Thesis, Taiyuan University of Technology (in Chinese).
  21. Zhao, J. *Experimental Study on the Microscopic Characteristics and Mechanical Properties of Oil Shale under High Temperature & Three-Dimensional Stress*. PhD Thesis, Taiyuan University of Technology (in Chinese).

*Presented by A. Konist*

Received April 8, 2019